Orthogonal Affine Invariants from Gaussian-Hermite Moments

Jan Flusser[1], Tomáš Suk[1(✉)], and Bo Yang[2]

[1] The Czech Academy of Sciences, Institute of Information Theory and Automation, Pod vodárenskou věží 4, 182 08 Praha 8, Czech Republic
{flusser,suk}@utia.cas.cz

[2] School of Automation, Northwestern Polytechnical University, 127 West Youyi Road, Xi'an 710 072, Shaanxi, People's Republic of China
bo.yang@hotmail.fr
https://www.utia.cas.cz

Abstract. We propose a new kind of moment invariants with respect to an affine transformation. The new invariants are constructed in two steps. First, the affine transformation is decomposed into scaling, stretching and two rotations. The image is partially normalized up to the second rotation, and then rotation invariants from Gaussian-Hermite moments are applied. Comparing to the existing approaches – traditional direct affine invariants and complete image normalization – the proposed method is more numerically stable. The stability is achieved thanks to the use of orthogonal Gaussian-Hermite moments and also due to the partial normalization, which is more robust to small changes of the object than the complete normalization. Both effects are documented in the paper by experiments. Better stability opens the possibility of calculating affine invariants of higher orders with better discrimination power. This might be useful namely when different classes contain similar objects and cannot be separated by low-order invariants.

Keywords: Affine transformation · Invariants · Image normalization · Gaussian-Hermite moments

1 Introduction

Recognition of objects that have undergone an unknown affine transformation has been the aim of extensive research work. The importance of affinely-invariant recognition techniques is mainly due to the fact, that 2D images are often projections of 3D world. As such, 2D images of 3D objects are perspective projections

This work has been supported by the Czech Science Foundation (Grant No. GA18-07247S) and by the Praemium Academiae, awarded by the Czech Academy of Sciences. Bo Yang has been supported by the Fundamental Research Funds for the Central Universities (No. 3102018ZY025) and the Fund Program for the Scientific Activities of the Selected Returned Overseas Professionals in Shaanxi Province (No. 2018024).

M. Vento and G. Percannella (Eds.): CAIP 2019, LNCS 11679, pp. 413–424, 2019.
https://doi.org/10.1007/978-3-030-29891-3_36

of their "ideal" views. Since perspective transformation is non-linear and difficult to cope with, in simplified imaging models it is often modelled by *affine transformation*. Such an approximation is justified if the object size is small comparing to the distance from the camera, because the perspective effect becomes negligible. For this reason, *affine invariants* play an important role in the view-independent object recognition and have been widely used not only in tasks where image deformation is intrinsically affine but also commonly substitute projective invariants.

Among the existing affine invariants, *moment invariants* are the most frequently studied, cited in the literature and used in applications (see [9] for an exhaustive survey). Their history can be traced back to Hilbert and other famous mathematicians of the last century [10,11,14,21,28,29], who elaborated the traditional theory of algebraic invariants. Currently, we may recognize two major approaches to the design of affine moment invariants (AMIs). In direct derivation, explicit formulas for the invariants are found by various techniques. Reiss [19] and Flusser and Suk [8] adopted the algebraic theory, Suk and Flusser applied graph theory [25,27] and Hickman proposed the method of transvectants [13]. All reported AMIs are composed of *geometric moments*, which are simple to work with theoretically but they are unstable in numerical implementation. When calculating them, we face the problem of precision loss due to the floating-point underflow and/or overflow. In theory of moments, a popular way of overcoming numerical problems is the use of orthogonal (OG) moments (i.e. moments defined as projections on an orthogonal polynomial basis) instead of the geometric ones. Since OG polynomials have a bounded range of values and can be calculated in a stable way by recurrent relations [4], the precision loss is by several orders less than that of geometric moments. Unfortunately, all known sets of OG polynomials are transformed under an affine transformation in so complicated manner, that a direct derivation of OG AMIs has not been reported yet.

Image normalization is an alternative way of obtaining invariants. The object is brought into certain canonical (also called normalized) position, which is independent of the actual position, rotation, scale, and skewing. The canonical position is usually defined by constraining the values of some moments, the number of which is the same as the number of free parameters of the transformation. Plain moments, calculated from the normalized object, are affine invariants of the original object. Affine image normalization was first proposed by Rothe et al. [20] and followed by numerous researchers [18,22,26,39].

Normalization approach seems to be attractive because of its simplicity. We can override the numerical problems by taking OG moments of the normalized image. Lin [16] used Chebyshev moments, Zhang [38] used Legendre moments, and Canterakis [3], Mei [17] and Amayeh [1] adopted Zernike moments for this purpose. Another advantage is that no actual spatial transformation of the original object is necessary. Such a transformation would slow down the process and would introduce resampling errors. Instead, the moments of the normalized object can be calculated directly from the original object using the normalization constraints. However, a major drawback of image normalization lies in the instability of the canonical position. Two visually very similar shapes may be brought, under the same normalization constraints, to distinct canonical positions. The difference in canonical positions propagates into all normalized moments and these shapes are no longer recognized as similar. This used to be the main argument against the normalization method.

In this paper, we propose an original "hybrid" approach, which should suppress the instability while keeping all the positive aspects of normalization, namely the possibility of working with OG moments. The main idea is to decompose affine transformation into anisotropic scaling and two rotations, normalize w.r.t. the first rotation and anisotropic scaling only, and then use moment invariants from OG moments w.r.t. the second rotation. Thanks to using OG moments, this method is numerically more stable than direct AMIs. At the same time, skipping the normalization w.r.t. the second rotation makes the canonical position robust to small changes of the object. Figure 1 shows the differences between these three approaches graphically.

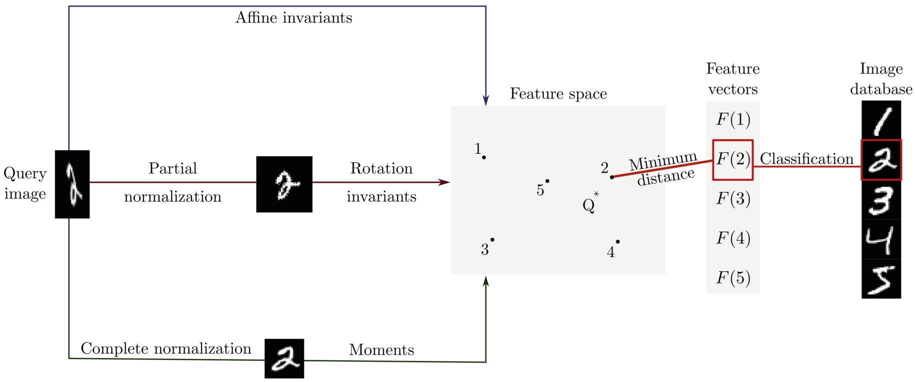

Fig. 1. Three approaches to reaching affine invariance. Direct affine invariants (top), partial normalization (middle), and complete normalization (bottom). We propose to use partial normalization followed by applying Gaussian-Hermite rotation invariants.

2 Affine Transformation and Its Decomposition

Affine transformation in 2D is defined as

$$\mathbf{x}' = \mathbf{A}\mathbf{x} + \mathbf{b} \tag{1}$$

where $\mathbf{A}$ is a regular 2×2 matrix with constant coefficients and $\mathbf{b}$ is a vector of translation. Normalization w.r.t. translation is achieved easily by shifting the coordinate origin into the object centroid. Thus, $\mathbf{b}$ vanishes and we will not consider it in the sequel.

Normalization w.r.t. $\mathbf{A}$ is based on a decomposition of $\mathbf{A}$ into a product of single-parameter matrices and subsequent normalizations w.r.t. each matrix.

Several decompositions can be used for this purpose. Rothe et al. [20] proposed two different decompositions – XSR decomposition into skewing, nonuniform scaling and rotation, and XYS decomposition into two skews and nonuniform scaling. Their method was later improved by Zhang [39], who studied possible ambiguities of the canonical position. Pei and Lin [18] tried to avoid the skewing matrix and proposed a decomposition into two rotations and a nonuniform scaling between them. A generalized and improved version of this decomposition was later published by Suk and Flusser [26]. We apply the decomposition scheme from [26] in this paper. We recall its basics below.

Affine matrix $\mathbf{A}$ is decomposed as

$$\mathbf{A} = \mathbf{R}_2\mathbf{T}\mathbf{R}_1\mathbf{S} \tag{2}$$

where $\mathbf{S}$ is a uniform scaling, $\mathbf{R}_1$ is the first rotation, $\mathbf{T}$ is so-called *stretching* which means $\mathbf{T}$ is diagonal and $T_{11} = 1/T_{22}$, and $\mathbf{R}_2$ is the second rotation. If $\mathbf{A}$ is regular, then such a decomposition always exists and is unique. If $\det(\mathbf{A}) < 0$, then $\mathbf{A}$ performs also a mirror reflection (flip) of the object and additional normalization to the mirror reflection is required. This case is however rare and we will not consider it in the sequel (we refer to [26] for detailed treatment of this case).

Now we apply the normalization from [26] but only to $\mathbf{S}$, $\mathbf{R}_1$ and $\mathbf{T}$. The normalization constraints are defined by prescribing the values of certain low order central moments. Moments of the original image are denoted as μ_{pq}, those of the normalized image as μ'_{pq}

$$\mu_{pq} = \int\int x^p y^q f(x,y)\mathrm{d}x\mathrm{d}y \tag{3}$$

(note that the image centroid has been already shifted to (0, 0)). Normalization to scaling $\mathbf{S}$ is constrained by $\mu'_{00} = 1$. Normalization to rotation $\mathbf{R}_1$ is achieved by the principal axis method (see [9], Chap. 3), when we diagonalize the second-order moment matrix and align the principal eigenvector with the x-axis. This is equivalent to constraints $\mu'_{11} = 0$ and $\mu'_{20} > \mu'_{02}$ and leads to the normalizing angle

$$\alpha = \frac{1}{2}\arctan\left(\frac{2\mu_{11}}{\mu_{20} - \mu_{02}}\right). \tag{4}$$

(If $\mu_{11} = 0$ and $\mu_{20} = \mu_{02}$, then we consider the image is already normalized to rotation and set $\alpha = 0$; if $\mu_{11} \neq 0$ and $\mu_{20} = \mu_{02}$, we set $\alpha = \pi/4$.) Normalization to stretching is done by imposing the constraint $\mu''_{20} = \mu''_{02}$.

In traditional "complete" normalization, the last normalization step – normalization w.r.t. $\mathbf{R}_2$ – is done by means of higher-order moments, which may lead to an unstable canonical position. An example of such instability is shown in Fig. 2. We used a T-like shape (we assumed it had already passed the normalization w.r.t. $\mathbf{S}$, $\mathbf{R}_1$ and $\mathbf{T}$) and varied its width t from 68 to 78 pixels. We normalized it w.r.t. rotation $\mathbf{R}_2$ by means of third-order moments as proposed in [26]. The canonical positions for $t = 68, 73$ and 78 pixels, respectively, are shown in Fig. 2 (b)–(d). We can see they differ from one another significantly, which leads to a strong discontinuity of any features calculated from the canonical form. In this paper, we propose to skip the last normalization and calculate rotation invariants from the canonical position achieved by normalization w.r.t. **S**, $\mathbf{R}_1$ and **T**. A similar idea was proposed by Heikkilä [12], who used Cholesky factorization of the second-order moment matrix for derivation of partial normalization constraints and then continued with geometric rotation moment invariants from [7].

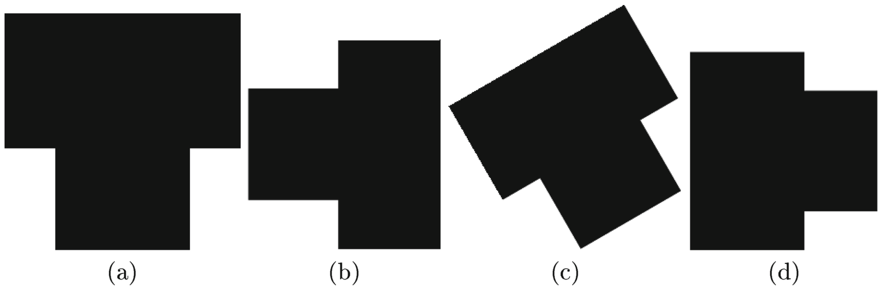

Fig. 2. The test shape of the thickness $t = 73$ before the normalization to $\mathbf{R}_2$ (a). The canonical positions after the $\mathbf{R}_2$-normalization has been applied for $t = 68$ (b), $t = 73$ (c), and $t = 78$ (d).

The rotation invariants we recommend to use are composed of Gaussian-Hermite (GH) moments. A brief introduction to GH moments along with an explanation why we chose GH moments for this purpose is given in the next section.

3 Gaussian–Hermite Moments and Invariants

Gaussian–Hermite moments and their use in image processing were exhaustively studied in [2,6,23,24,30,32–34,36]. Hermite polynomials are defined as

$$H_p(x) = (-1)^p \exp(x^2) \frac{d^p}{dx^p} \exp(-x^2). \tag{5}$$

They are orthogonal on $(-\infty, \infty)$ with a Gaussian weight function

$$\int_{-\infty}^{\infty} H_p(x) H_q(x) \exp(-x^2) dx = 2^p p! \sqrt{\pi} \delta_{pq} \tag{6}$$

and they can be efficiently computed by the following three-term recurrence relation

$$H_{p+1}(x) = 2x H_p(x) - 2p H_{p-1}(x) \quad \text{for } p \geq 1, \tag{7}$$

with the initial conditions $H_0(x) = 1$ and $H_1(x) = 2x$. For the definition of Gaussian–Hermite moments, we scale Hermite polynomials by a parameter σ and modulate them by a Gaussian function with the same parameter. Hence, the Gaussian–Hermite moment (GHM) $\overline{\eta}_{pq}$ of image $f(x, y)$ is defined as

$$\overline{\eta}_{pq} = \int\limits_{-\infty}^{\infty}\int\limits_{-\infty}^{\infty} H_p\left(\frac{x}{\sigma}\right) H_q\left(\frac{y}{\sigma}\right) \exp\left(-\frac{x^2+y^2}{2\sigma^2}\right) f(x,y)\mathrm{d}x\mathrm{d}y. \tag{8}$$

The most important property of the GHMs for object recognition, making them "prominent" OG moments, is the following one. GHMs are transformed under an image rotation in the same way as geometric moments. In particular, given a functional $I(f, \mu_{pq}), \quad p, q = 0, 1, \cdots, r$ which is invariant under rotation of image f, then functional $I(f, \overline{\eta}_{pq})$ is also an invariant. This theorem was discovered by Yang et al. [36]. Recently, the proof has been given in [31] that GHMs are the only orthogonal polynomials possessing this property. The Yang's theorem offers an easy and elegant way to design rotation invariants from GHMs of arbitrary orders [34]. In the classical geometric moment invariants from [7] that were proven to form an independent and complete set

$$\begin{aligned} \Phi_{pq} = &\left(\sum_{k=0}^{q_0}\sum_{j=0}^{p_0}\binom{q_0}{k}\binom{p_0}{j}(-1)^{p_0-j}i^{p_0+q_0-k-j}\mu_{k+j,p_0+q_0-k-j}\right)^{p-q} \\ &\cdot\sum_{k=0}^{p}\sum_{j=0}^{q}\binom{p}{k}\binom{q}{j}(-1)^{q-j}i^{p+q-k-j}\mu_{k+j,p+q-k-j} \end{aligned} \tag{9}$$

where $p \geq q$ and p_0, q_0 are fixed user-defined indices such that $p_0 - q_0 = 1$, we only replace all μ_{pq}'s with corresponding $\overline{\eta}_{pq}$'s. These invariants are finally applied to the partially normalized image.

The idea of partial normalization is not fixed to any particular type of moments. In principle, any moments generating rotation invariants could be employed here. However, our experiments show that the GHMs perform better than all tested alternatives. We could use, similarly to [12], directly geometric moment invariants (9) but OG moments in general ensure better numerical stability and hence offer the possibility of using higher-order invariants [9]. Among OG moments, the moments orthogonal on a unit circle such as Zernike and Fourier-Mellin moments, provide an immediate rotation invariance and could be used here as well. Their application, however, requires mapping the image inside the unit circle, which introduces additional errors due to resampling and requires an extra time. So, moments orthogonal on a square appear to be an optimal choice because they are inherently suitable to work on a pixel grid directly. Finally, as proved in [31], GHMs are the only moments orthogonal on a square and yielding rotation invariants in the explicit form[1]. In this sense, GHMs provide an optimal solution.

4 Partial Normalization Method

In this section, we present the entire method step by step.

1. Let $f(x, y)$ be an input image, possibly deformed by unknown affine transformation $\mathbf{A}$. Compute the normalization parameters w.r.t. partial matrices $\mathbf{S}$, $\mathbf{R}_1$ and $\mathbf{T}$ as described in Sect. 2. Do not transform/resample the image $f(x, y)$, do not generate the normalized image $f'(x, y)$.
2. Calculate the transformed coordinates

$$\begin{pmatrix} x' \\ y' \end{pmatrix} = \mathbf{T}\mathbf{R}_1\mathbf{S} \begin{pmatrix} x \\ y \end{pmatrix}. \tag{10}$$

3. Calculate the GHMs (8) of the original image $f(x, y)$ with the Gaussian-Hermite polynomials computed on the normalized coordinates from the previous step. To do so, we have to know how GH polynomials are transformed under rotation and scaling. Fortunately, both relations are well known: GHMs are under rotation transformed as geometric moments [36]

$$\overline{\eta}'_{pq} = \sum_{k=0}^{p} \sum_{j=0}^{q} \binom{p}{k} \binom{q}{j} (-1)^j \ \sin^{p-k+j} \alpha \ \cos^{q+k-j} \alpha \ \overline{\eta}_{k+j,p+q-k-j}. \tag{11}$$

   The behavior of GHMs under scaling was analyzed in [35]. Scaling affects not only the coordinates of Hermite polynomials but also the variance of the Gaussian modulation, which must be compensated by dividing the coordinates by $\sqrt{\mu_{00}}$. Since scaling is separable, we need just a 1D transformation for both 2D scaling and stretching. Thanks to this, we obtain the GHMs of $f'(x, y)$ without actually creating the normalized image.
4. Substitute the GHMs into (9) and calculate Gaussian-Hermite affine moment invariants (GHAMIs) of $f(x, y)$. They constitute the feature vector for invariant image description and classification.

5 Numerical Experiment

In this section, we test how the GHAMIs perform numerically and compare them to their two closest competitors, which are direct AMIs from geometric moments

[1] The reader may recall the so-called "indirect approach" to constructing rotation invariants from Legendre [5,15] and Krawtchouk [37] moments. The authors basically expressed geometric moments in terms of the respective OG moments and substituted into (9). They ended up with clumsy formulas of questionable numerical properties.

(a) (b)

Fig. 3. Original test images: (a) Lena, (b) Lisa.

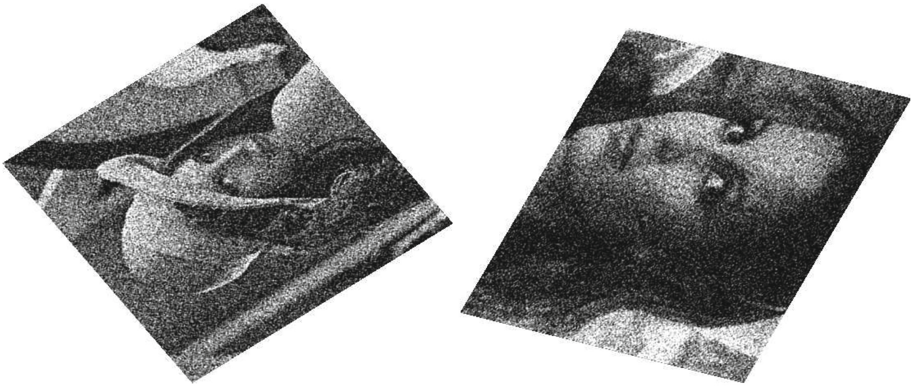

(a) (b)

Fig. 4. Examples of the transformed and noisy test images: (a) Lena, (b) Lisa.

by Reiss and Suk [19,27] and partial normalization along with rotation invariants by Heikkila [12]. We choose direct AMIs for comparison since they are well-established and most cited affine invariants based on moments. Heikkila's method was chosen because it uses a similar idea of a partial normalization as we do. Comparison to other affine invariant methods is mostly irrelevant or unfair. For instance, the instability of complete normalization methods illustrated in Fig. 2 so much degrades their invariants, that these methods are seriously handicapped, even if the instability occurs on certain objects only. That is why we did not include any complete normalization method in this experimental study. We took two commonly used test images (see Fig. 3), generated 200 random affine transformations of both and added heavy Gaussian white noise of SNR = 0 dB to every image (see Fig. 4 for an example). For each image, we calculated a complete set of invariants up to the 12th moment order by three methods mentioned

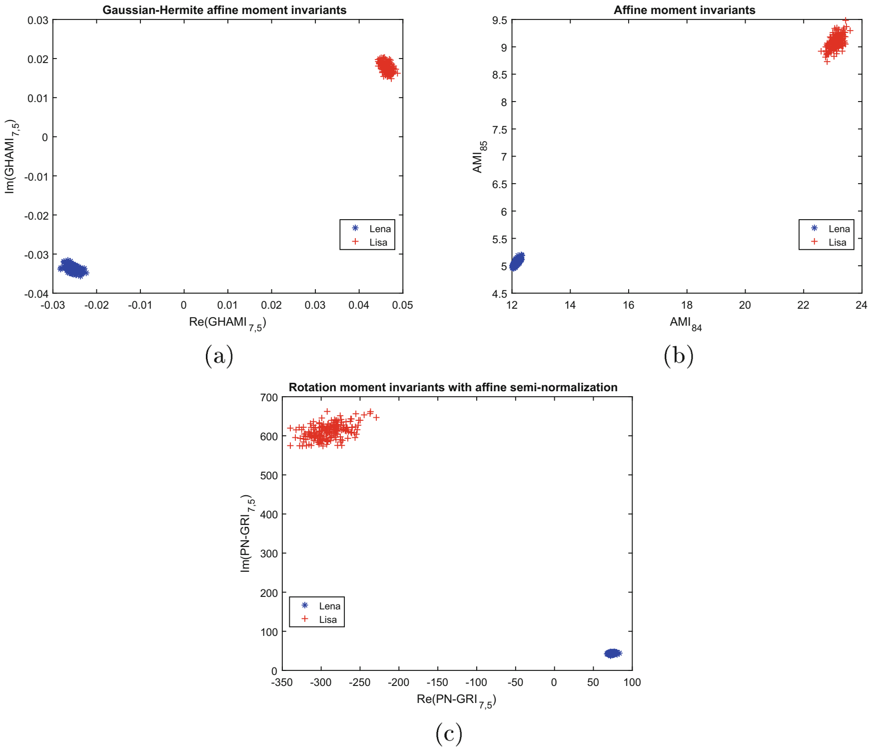

Fig. 5. The subspaces of two invariants of order 12 out of 85 invariants calculated: (a) GHAMIs, (b) AMIs, (c) PN-GRIs.

above. We choose the order 12 as a compromise – it allows to demonstrate the higher-order properties while still being numerically tractable. The complete set up to the 12th order consists of 85 independent invariants.

As a quality criterion, we chose the between-class separability measured by Mahalanobis distance

$$M = \sqrt{(\mathbf{m}_1 - \mathbf{m}_2)^T (\mathbf{S}_1 + \mathbf{S}_2)^{-1} (\mathbf{m}_1 - \mathbf{m}_2)}, \tag{12}$$

where $\mathbf{m}_i$ is the class mean and $\mathbf{S}_i$ is the covariance matrix. To demonstrate the higher-order effects, we used only the invariants of the highest (i.e. the 12th in this case) order. There are 13 invariants of the 12th order in each method.

The best separability was achieved by the proposed method using GHAMIs ($M = 173$), the worst one was provided by partial normalization and geometric rotation invariants (PN-GRIs, $M = 103$), and the AMIs performed somewhere in between yielding $M = 131$. The best performance of the GHAMIs is because the geometric moments, employed in the other two reference methods, suffer from the precision loss when calculating higher-order moments. The subspaces of two invariants are shown in Fig. 5 for illustration. It should be noted, that the separability in the case of GHAMIs is influenced by the modulation parameter σ. We tested several settings and found out that $\sigma = 0.525$ maximizes the Mahalanobis distance between these images.

While for the evaluation by Mahalanobis distance between two classes we used only the invariants of order 12, the graphs in Fig. 6 show how the dispersion of an individual class grows as the moment order increases from 3 to 12. We can see that the growth of the mean standard deviation has an exponential character for AMIs and PN-GRIs, while staying reasonably low in the case of GHAMIs. To make this comparison as fair as possible, we compensated the differences in the range of values by dividing of the AMIs values by 10 and those of the PN-GRIs by 100.

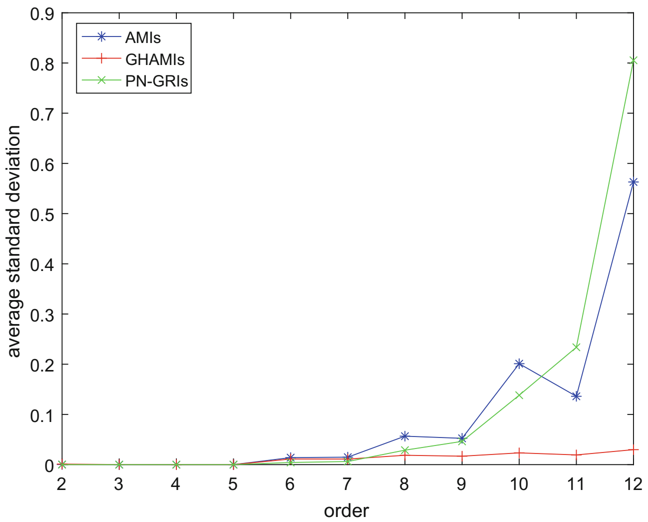

Fig. 6. Mean standard deviations of the GHAMIs, AMIs, and geometric rotation moment invariants for the Lena cluster. The average was calculated over all invariants of each order. Note the rapid growth of AMIs and PN-GRIs caused by the precision loss.

6 Conclusion

We proposed a new kind of moment invariants w.r.t. affine transformation. The new invariants are constructed in two steps. First, the image is partially normalized up to a rotation, and then recently proposed rotation invariants from Gaussian-Hermite moments are applied. Comparing to the existing approaches – direct affine invariants and complete normalization - the proposed method is more numerically stable and opens the possibility of using affine invariants of higher orders than before. This might be useful namely when different classes contain similar objects and cannot be separated by low-order invariants.

References

1. Amayeh, G., Kasaei, S., Bebis, G., Tavakkoli, A., Veropoulos, K.: Improvement of Zernike moment descriptors on affine transformed shapes. In: 9th International Symposium on Signal Processing and Its Applications ISSPA 2007, pp. 1–4. IEEE (2007)
2. Belghini, N., Zarghili, A., Kharroubi, J.: 3D face recognition using Gaussian Hermite moments. Int. J. Comput. Appl. Spec. Issue Softw. Eng., Databases Expert. Syst. **SEDEX**(1), 1–4 (2012)
3. Canterakis, N.: 3D Zernike moments and Zernike affine invariants for 3D image analysis and recognition. In: Ersbøll, B.K., Johansen, P. (eds.) Proceedings of the 11th Scandinavian Conference on Image Analysis SCIA 1999. DSAGM (1999)
4. Chihara, T.S.: An Introduction to Orthogonal Polynomials. Gordon and Breach, New York (1978)
5. Deepika, C.L., Kandaswamy, A., Vimal, C., Satish, B.: Palmprint authentication using modified Legendre moments. Procedia Comput. Sci. **2**, 164–172 (2010). Proceedings of the International Conference and Exhibition on Biometrics Technology ICEBT'10
6. Farokhi, S., Sheikh, U.U., Flusser, J., Yang, B.: Near infrared face recognition using Zernike moments and Hermite kernels. Inf. Sci. **316**, 234–245 (2015)
7. Flusser, J.: On the independence of rotation moment invariants. Pattern Recognit. **33**(9), 1405–1410 (2000)
8. Flusser, J., Suk, T.: Pattern recognition by affine moment invariants. Pattern Recognit. **26**(1), 167–174 (1993)
9. Flusser, J., Suk, T., Zitová, B.: 2D and 3D Image Analysis by Moments. Wiley, Chichester (2016)
10. Grace, J.H., Young, A.: The Algebra of Invariants. Cambridge University Press, Cambridge (1903)
11. Gurevich, G.B.: Foundations of the Theory of Algebraic Invariants. Nordhoff, Groningen (1964)
12. Heikkilä, J.: Pattern matching with affine moment descriptors. Pattern Recognit. **37**, 1825–1834 (2004)
13. Hickman, M.S.: Geometric moments and their invariants. J. Math. Imaging Vis. **44**(3), 223–235 (2012)
14. Hilbert, D.: Theory of Algebraic Invariants. Cambridge University Press, Cambridge (1993)
15. Hosny, K.M.: New set of rotationally Legendre moment invariants. Int. J. Electr. Comput. Syst. Eng. **4**(3), 176–180 (2010)
16. Liu, Q., Zhu, H., Li, Q.: Image recognition by affine Tchebichef moment invariants. In: Deng, H., Miao, D., Lei, J., Wang, F.L. (eds.) AICI 2011, Part III. LNCS (LNAI), vol. 7004, pp. 472–480. Springer, Heidelberg (2011). https://doi.org/10.1007/978-3-642-23896-3_58
17. Mei, Y., Androutsos, D.: Robust affine invariant shape image retrieval using the ICA Zernike moment shape descriptor. In: 16th IEEE International Conference on Image Processing (ICIP), pp. 1065–1068, November 2009
18. Pei, S.C., Lin, C.N.: Image normalization for pattern recognition. Image Vis. Comput. **13**(10), 711–723 (1995)
19. Reiss, T.H.: The revised fundamental theorem of moment invariants. IEEE Trans. Pattern Anal. Mach. Intell. **13**(8), 830–834 (1991)

20. Rothe, I., Süsse, H., Voss, K.: The method of normalization to determine invariants. IEEE Trans. Pattern Anal. Mach. Intell. **18**(4), 366–376 (1996)
21. Schur, I.: Vorlesungen über Invariantentheorie. Springer, Berlin (1968). https://doi.org/10.1007/978-3-642-95032-2. in German
22. Shen, D., Ip, H.H.S.: Generalized affine invariant image normalization. IEEE Trans. Pattern Anal. Mach. Intell. **19**(5), 431–440 (1997)
23. Shen, J.: Orthogonal Gaussian-Hermite moments for image characterization. In: Casasent, D.P. (ed.) Intelligent Robots and Computer Vision XVI: Algorithms, Techniques, Active Vision, and Materials Handling, vol. 3208, pp. 224–233. SPIE (1997)
24. Shen, J., Shen, W., Shen, D.: On geometric and orthogonal moments. Int. J. Pattern Recognit. Artif. Intell. **14**(7), 875–894 (2000)
25. Suk, T., Flusser, J.: Graph method for generating affine moment invariants. In: Proceedings of the 17th International Conference on Pattern Recognition ICPR 2004, pp. 192–195. IEEE Computer Society (2004)
26. Suk, T., Flusser, J.: Affine normalization of symmetric objects. In: Blanc-Talon, J., Philips, W., Popescu, D., Scheunders, P. (eds.) ACIVS 2005. LNCS, vol. 3708, pp. 100–107. Springer, Heidelberg (2005). https://doi.org/10.1007/11558484_13
27. Suk, T., Flusser, J.: Affine moment invariants generated by graph method. Pattern Recognit. **44**(9), 2047–2056 (2011)
28. Sylvester assisted by F. Franklin, J.J.: Tables of the generating functions and groundforms for simultaneous binary quantics of the first four orders taken two and two together. Am. J. Math. **2**, 293–306, 324–329 (1879)
29. Sylvester assisted by F. Franklin, J.J.: Tables of the generating functions and groundforms for the binary quantics of the first ten orders. Am. J. Math. **2**, 223–251 (1879)
30. Yang, B., Dai, M.: Image analysis by Gaussian-Hermite moments. Signal Process. **91**(10), 2290–2303 (2011)
31. Yang, B., Flusser, J., Kautsky, J.: Rotation of 2D orthogonal polynomials. Pattern Recognit. Lett. **102**(1), 44–49 (2018)
32. Yang, B., Flusser, J., Suk, T.: Steerability of Hermite kernel. Int. J. Pattern Recognit. Artif. Intell. **27**(4), 1–25 (2013)
33. Yang, B., Flusser, J., Suk, T.: 3D rotation invariants of Gaussian-Hermite moments. Pattern Recognit. Lett. **54**(1), 18–26 (2015)
34. Yang, B., Flusser, J., Suk, T.: Design of high-order rotation invariants from Gaussian-Hermite moments. Signal Process. **113**(1), 61–67 (2015)
35. Yang, B., Kostková, J., Flusser, J., Suk, T.: Scale invariants from Gaussian-Hermite moments. Signal Process. **132**, 77–84 (2017)
36. Yang, B., Li, G., Zhang, H., Dai, M.: Rotation and translation invariants of Gaussian-Hermite moments. Pattern Recognit. Lett. **32**(2), 1283–1298 (2011)
37. Yap, P.T., Paramesran, R., Ong, S.H.: Image analysis by Krawtchouk moments. IEEE Trans. Image Process. **12**(11), 1367–1377 (2003)
38. Zhang, H., Shu, H., Coatrieux, G., Zhu, J., Wu, J., Zhang, Y., Zhu, H., Luo, L.: Affine Legendre moment invariants for image watermarking robust to geometric distortions. IEEE Trans. Image Process. **20**(8), 2189–2199 (2011)
39. Zhang, Y., Wen, C., Zhang, Y., Soh, Y.C.: On the choice of consistent canonical form during moment normalization. Pattern Recognit. Lett. **24**(16), 3205–3215 (2003)